Received: 26 February 2019 | Revised: 6 July 2019 | Accepted: 23 July 2019

DOI: 10.1002/aoc.5175

FULL PAPER

WILEY Applied Organometallic Chemistry

Structural and theoretical studies of the methoxycarbonylation of higher olefins catalysed by (Pyrazolyl-ethyl)pyridine palladium (II) complexes

Siyabonga Zulu | Mohd.G. Alam[†] | Stephen O. Ojwach | Matthew P. Akerman

School of Chemistry and Physics, Pietermaritzburg Campus, University of KwaZulu-Natal, Private Bag X01, Scottsville 3209, South Africa

Correspondence
Stephen O. Ojwach, School of Chemistry and Physics, Pietermaritzburg Campus, University of KwaZulu-Natal, Private Bag X01. Scottsville 3209, South Africa.
Email: ojwach@ukzn.ac.za

Present Address
[†]Department of Industrial Chemistry, Addis Ababa Science and Technology University, P. O. Box, 16417, Addis Ababa, Ethiopia

Funding information
National Research Foundation South Africa, Grant/Award Number: CPRR98938; University of KwaZulu-Natal; NRF-South Africa, Grant/Award Number: CPRR-98938; NRF-DST (South Africa) Centre of Excellence

Reactions of 2-[1-(3,5-dimethylpyrazol-1-yl)ethyl]pyridine **(L1)** and 2-[1-(3,5-diphenylpyrazol-1-yl)ethyl]pyridine **(L2)** with the [Pd (COD)Cl_2] or [Pd (COD)MeCl] produced palladium (II) complexes [Pd(**L1**)ClMe] (**1**), [Pd(**L1**)Cl_2] (**C2**), [Pd(**L2**)ClMe] (**3**), and [Pd(**L2**)Cl_2] (**4**) in quantitative yields. Solid state structures of complexes **1**, **3** and **4** established the formation of mononuclear compounds, containing one bidentate ligand unit per metal atom, to give square planar complexes. All the other spectroscopic characterization data and elemental analyses were consistent with the observed structures. All the palladium (II) complexes **1–4** gave active catalysts in the methoxycarbonylation of 1-octenes. The catalysts demonstrated 100% chemoselectivities towards esters and favored the formation of linear isomers. Reaction conditions such as the type of phosphine derivative, acid promoter, solvent system, time, pressure and temperature have been investigated and shown to affect both the catalytic activity and regio-selectivity of the catalysts. Solid-angle modelling established the comparable steric contributions from the ligands, consistent with the similar regioselectivities of the resultant catalysts.

KEYWORDS
methoxycarbonylation, modelling, olefins, palladium, structures

1 | INTRODUCTION

Transition metal catalyzed olefin transformation reactions are among the key applications of transition metal catalysts in industrial processes.[1] Examples include olefin oligomerization,[2] polymerization[3] hydrogenation[4] and oxidation[5] reactions among others. Among the metal complexes, palladium systems represent a huge proportion of the industrially used catalysts. This attribute is due to the versatility of the palladium complexes, in terms of catalytic activity, selectivity and stability. There is no better illustration of this versatility than in the use of palladium complexes as catalysts in carbon–carbon coupling reactions such as Heck[6] and Suzuki-Miyaura[7] coupling reactions.

Another olefin transformation reaction where palladium complexes have gained much prominence is the methoxycarbonylation of olefins.[8] Methoxycarbonylation of olefins is an attractive industrial synthetic strategy due to the inherent production of useful commodities such as pharmaceuticals, perfumes, surfactants and fragrances.[1,9] Traditionally, phosphine-based palladium complexes have been used in these reactions and still remain the most superior catalysts.[10,11] To date, the main approach has been the use of *in situ* generated palladium catalysts, by adding phosphine-ligands to the palladium metal salts. While these systems remain the

catalysts of choice in methoxycarbonylation reactions, they suffer from several drawbacks, such as high costs of phosphine-based catalysts, difficulty in their syntheses and lack of understanding of the exact active species. Thus, there has been a surge in the search for cheaper, well-defined and discrete metal complexes that could rival these phosphine systems.

This has seen the emergence of N^P, N^O and N^N donor palladium catalysts as suitable replacements of the well-established phosphine-based catalysts. Notable examples include, the N^P palladium complexes, reported by Aguirre and co-workers, which showed promising results with respect to region-selectivities and catalytic activities.[12] In another piece of work, Chaudhari and co-workers used cationic N^O palladium systems which also display remarkable catalytic performance.[13] Based on the promising results we have obtained for the past decade using pyrazolyl transition metal catalysts in various olefin transformation reactions,[14] we opted to investigate the ability of these types of complexes in the methoxycarbonylation of higher olefins.

Thus in this contribution, we report a modified (pyrazolylethyl)pyridine ligand design to the one we recently used in the methoxycarbonylation of olefins.[15] The motivation for the incorporation of a methyl group in the methylene bridge was to introduce chirality at the methylene carbon for possible application in asymmetric methoxycarbonylation catalysis. However, as we previously discussed,[16] only racemic mixtures of the ligand were obtained. In this current work, we therefore report the syntheses of palladium (II) complexes of these ligands, their structural characterization and applications as catalysts in methoxycarbonylation of higher olefins. The dependence of catalyst performance on ligand structure, nature of acid promoter, type of phosphine stabilizer and olefin substrate, under different reactions conditions, have been investigated. Density Functional Theoretical studies and solid angle modelling have also been performed to offer insights into the experimental trends observed.

2 | RESULTS AND DISCUSSION

2.1 | Syntheses and spectroscopic characterization of palladium complexes

Ligands 2-[1-(3,5-dimethylpyrazol-1-yl)ethyl]pyridine (**L1**) and 2-[1-(3,5-diphenylpyrazol-1-yl)ethyl]pyridine (**L2**) were prepared following our recently published procedures.[16] Reactions of synthons 2-[1-(3,5-dimethylpyrazol-1-yl)ethyl]pyridine **(L1)** and 2-[1-(3,5-diphenylpyrazol-1-yl)ethyl]pyridine **(L2)** with the [Pd (COD)Cl_2] or [Pd (COD)ClMe] metal salts produced the corresponding neutral complexes **1–4** as brown solids in low to good yields (44%–84%) as shown in Scheme 1. All the compounds were characterized using ^{1}H NMR, ^{13}C NMR, FT-IR, mass spectroscopy, elemental analysis, and single crystal X-ray crystallography for **L2**, complexes **1**, **2** and **4**. As previously reported for the nickel complexes[16] the palladium complexes (**1–4**) were racemic mixtures and hence no *R*/*S* enantiomers were resolved.

Comparison of the ^{1}H NMR and ^{13}C NMR spectra of the ligands and the respective palladium complexes, allowed us to establish successful complex formation. For instance, the methylene methyl protons were recorded at 1.56 ppm and 1.94 ppm in ligand **L1** and its corresponding complex **1**, respectively (Figure S1). The additional signal recorded up field at 0.95 ppm in complex **1** was assigned to the Pd-CH_3 protons and further established the isolation of the desired compound. Corroborative evidence was also obtained from the ^{13}C NMR spectra where the methylene carbon was reported at 59.1 ppm and 58.7 ppm in **L1** and **2**, respectively (Figure S2). IR spectroscopy was also used to determine the identities of complexes **1–4**. Typical IR frequencies for C=N_{pz} and C=N_{py} were reported in the range of 2162 cm^{-1}-2164 cm^{-1} and 1605 cm^{-1}-2112 cm^{-1}. A downfield shift of the C=N_{pz} peak from 1975 cm^{-1} to 2164 cm^{-1} for ligand **L1** and its corresponding complex **4** respectively (Figure S3), established the coordination of ligand to the palladium atom.[17,18] Mass spectral data of the complexes were also used to deduce their identities. For example, mass spectrum of complex **4** (Figure S4), showed an m/z signal at 503.1116 amu, corresponding to the molecular ion (Mw = 502.73 g/mol). The loss of the two phenyl groups on the pyrazolyl motif gave a base peak at m/z = 348.1805 amu. Elemental analyses data of complexes **1–4** tallied with the presence of one ligand unit per palladium metal atom as depicted in Scheme 1, and also confirmed the purity of the bulk materials.

2.2 | Molecular structures of compounds L2, 1, 3 and 4

The structures of the palladium (II) complexes **1**, **2** and **4** as well as the free ligand **L2** were elucidated using single crystal X-ray diffraction methods. The displacement

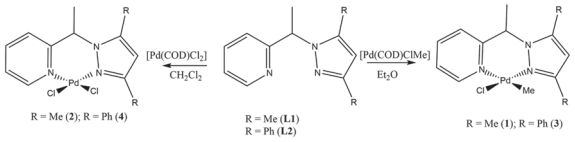

SCHEME 1 Syntheses of 2-(pyrazolyl-ethyl)-pyridine palladium (II) complexes 1–4.

ellipsoid plots for compounds **L2**, **1**, **2** and **4** are shown in Figure 1, while Tables 1 and 2 contain data collection and crystallographic parameters and selected bond lengths and bond angles of the compounds respectively. Compound **L2** crystallized in the monoclinic space group $P2_1/n$ with a single molecule in the asymmetric unit and $Z = 4$. The ligand geometry in many respects remains unchanged when chelated to the Pd (II) metal center. The key difference is the relative geometry of the pyridyl ring. This rotation is illustrated by the N1–C5–N3–N2 torsion angle which measures 110.4(2)° in the ligand. Rotation about the C5–C6 bond is therefore required for metal ion chelation. Complex **1** crystallizes in a mixture of two isomers in a 3:1 ratio and showed positional disorder in relation to the chloride and methyl ligands. The isomer with the chloride ligand *cis* to the pyridyl N atom is dominant, with a site occupancy of 75%. The minor isomer has the methyl ligand *cis* to the pyridyl N atom (site occupancy 25%). Despite complex **1** crystallizing in a mixture of isomers (3:1), only one set of the signals is observed in the ^{1}H NMR spectra (Figure S1), which can be assigned to the two being thermodynamic isomers rather than kinetic in nature.

Density functional theory (DFT) simulations were used to gain a deeper understanding of the solid-state structures and relative energies of the different conformers of the compounds **1** and **3**. Least squares fits of the experimental solid state structures and lowest energy DFT-simulated structures are shown in Figure S5. The similarity of the structures as measured by the root-mean-square deviations show that the structures are in good agreement. The relative energies of the two conformers confirmed that the dominant form in the solid state is lower in energy (Figure S6). Indeed, the energy difference between the major isomer (observed) and the minor isomer of 8.82 kJ/mol (Figure S6) is large enough to explain the observation of one set of signals in the ^{1}H NMR spectra of complex **2**. The three metal complexes all show nominally square planar coordination geometries, consistent with the group congener platinum (II) and is a consequence of the d^8 electronic configuration associated vacant dx^2-y^2 orbitals. Coordination of the bidentate pyrazole-pyridyl ligand yields a six-membered coordination ring.

The data in Table 2 clearly illustrate the approximately square planar coordination geometry of the metal ion with only small deviations from ideality imposed by the ligand geometry in some cases. The bond lengths and angles are in good agreement with those previously reported for comparable asymmetric palladium (II) complexes.[19–22] The most significant deviation from the ideal bond angle of 90° is the N–Pd–N bond angle which averages 86.65(12)°. Coordination of the ligand to the metal forms a six-membered ring which allows the bond to approach the ideal angle compared to the more common five-membered rings, which shows significantly more acute angles.[20] On the hand, the N–Pd–Cl bond angles are slightly obtuse. This angle is not limited by ligand geometry and the larger bond angle would minimize the non-bonded repulsion between the *ortho* phenyl C–H and methyl hydrogen atoms. The sp^3 hybridized carbon atom joining the pyridyl and pyridine rings leads to a usual chelate geometry. Although the four atoms coordinated to the metal ion are co-planar, the ligand itself is distinctly dome-shaped as a consequence of the sp^3 hybridized carbon (Figure S7). The absence of classical hydrogen bond donors from the three metal complexes precludes strong hydrogen bonding interactions (Table S1). However, the chloride ligand enables the formation of stabilizing intermolecular C–H···Cl interactions (Figures S8-S11).

2.3 | Methoxycarbonlyation of higher olefins catalysed by complexes 1–4

Complexes **1–4** were screened in the methoxycarbonylation of olefins using 1-octene as the

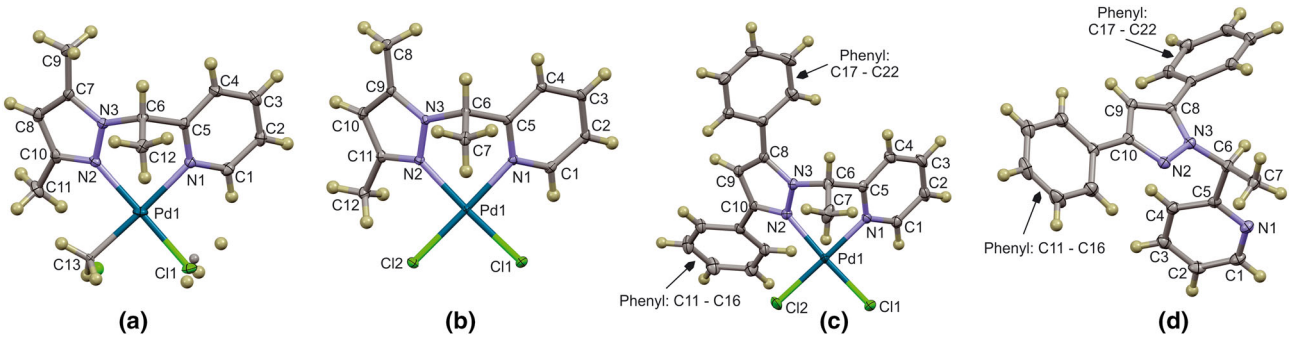

FIGURE 1 Displacement ellipsoid plot (50% probability surfaces) for the Pd (II) complexes (a) 1, (b) 2, (c) 4 and ligand (d) L2. The Pd (II) complexes all show a comparable nominally square planar coordination geometry. All data were collected at 100 K. The hydrogen atoms as well as the atoms of the minor component of complex (1) have been displayed with arbitrary radii

TABLE 1 Crystal data and structure refinement details for the Pd (II) complexes **1**, **2**, **4** and ligand **L2**

Crystal Data	1	2	4	L2
Chemical formula	$C_{13}H_{18}ClN_3Pd$	$C_{12}H_{15}Cl_2N_3Pd$	$C_{22}H_{19}Cl_2N_3Pd$	$C_{22}H_{19}N_3$
Molar mass (g mol^{-1})	358.15	378.57	502.70	325.40
Crystal system, space group	Orthorhombic, $P2_12_12_1$	Triclinic, *P*-1	Triclinic, *P*-1	Monoclinic, $P2_1/n$
Temperature (K)	100(2)	100(2)	100(2)	100(2)
a, *b*, *c* (Å)	7.254(1), 12.410(1), 15.2824(15)	8.185(5), 8.562(5), 11.245(5)	10.736(5), 10.936(5), 12.390(5)	8.348(2), 13.852(2), 15.587(3)
α, β, γ (^{0})	90, 90, 90	71.195(5), 87.246(5), 69.290(5)	114.985(5), 97.083(5), 104.375(5)	90, 103.257(4), 90
V (Å^3)	1375.7(2)	695.8(7)	1233.4	1754.5(5)
Z	4	2	2	4
Radiation type	Mo *Kα*			
μ (mm^{-1})	1.53	1.70	0.98	0.07
Crystal size (mm)	0.22 × 0.09 × 0.06	0.42 × 0.08 × 0.04	0.70 × 0.31 × 0.15	0.46 × 0.25 × 0.11
Data Collection				
Diffractometer	Bruker APEXII CCD diffractometer			
Absorption correction	Multi-scan, SADABS			
T_{min}, T_{max}	0.669, 0.746	0.666, 0.745	0.657, 0.745	0.958, 0.998
No. of measured, independent and observed [$I > 2\sigma$(I)] reflections	20525, 3395, 3368	22403, 2701, 2634	30530, 4845, 4716	14539, 3413, 3095
R_{int}	0.028	0.024	0.23	0.021
Refinement				
$R[F^2 > 2\sigma(F^2)]$, $wR(F^2)$, *S*	0.017, 0.041, 1.13	0.014, 0.034, 1.04	0.021, 0.049, 1.06	0.037, 0.091, 1.07
No. of reflections	3395	2701	4845	3413
No. of parameters	178	166	254	227
H-atom treatment	H-atom parameters constrained			
$\Delta\rho_{max}$, $\Delta\rho_{min}$ (e Å^{-3})	0.54, −0.51	0.41, −0.37	0.85, −0.88	0.25, −0.19

model substrate at 90 °C, 60 bar of CO, PPh_3 as the stabilizer and HCl as the acid promoter. The [Pd]/[PPh_3]/[HCl]/[1-octene] ratio of 1/2/10/200 in methanol/toluene solvent mixture was employed (Scheme 2). The results obtained for complexes **1**–**4** (Figure 2) showed that the complexes form active catalysts giving percentage conversion of 81%–91% within 24 hr. Generally, all the complexes afforded 100% chemoselectivity towards esters and regioselectivity of 51%–58% for the linear esters. Typical GC and GC–MS spectra of the methoxycarbonylation products are shown in Figures S12 and S13 respectively.

In terms of the effect of complex structure, there was a slight impact of ligand architecture on the catalytic activities. For instance, complexes **2** and **4**, bearing methyl **(L1)** and phenyl (**L2**) substituents on the pyrazolyl motif afforded conversions of 91% and 84%, respectively. Similarly, complexes **1 (L1)** and **3 (L2)** gave conversions of 86% and 82%, indicating that increased steric hindrance around the palladium metal resulted in diminished catalytic activities. The role of the phenyl substituents may be two-fold; steric encumbrance and increased electron donation leading to reduced electrophilicity of the metal center. In both cases, substrate coordination to the metal center would be hindered.[23] The Pd-Cl/Me groups also showed some marginal influence in the catalytic activities, with complex **2** bearing Pd-Cl showing higher conversions(91%) compared to its analogous Pd-Me complex **1** (86%). This has been previously reported by other researchers[24] and may be associated with the lower stability of the Pd-Me complexes, and/or reactive Pd-Cl in the formation of the Pd-hydride active intermediate.[25]

With respect to regioselectivity, there was no significant variation in the composition of either branched or linear esters with the pyrazolyl substituent. One would expect higher composition of the branched esters for

TABLE 2 Selected bond parameters for complexes **1**, **2** and **4**

Bond	Length (Å)	Bond	Angle (°)
1			
Pd1–Cl1	2.276(2)	Cl1–Pd1–N1	93.79(7)
Pd1–N1	2.131(2)	N1–Pd1–N2	87.11(8)
Pd1–N2	2.059(2)	N2–Pd1–C13	90.80(10)
Pd1–C13	2.106(5)	Cl1–Pd1–C13	88.30(10)
2			
Pd1–Cl1	2.290(1)	Cl1–Pd1–N1	90.92(4)
Pd1–Cl2	2.296(1)	N1–Pd1–N2	86.56(6)
Pd1–N1	2.029(2)	N2–Pd1–Cl2	92.79(4)
Pd1–N2	2.022(2)	Cl2–Pd1–Cl1	89.68(2)
4			
Pd1–Cl1	2.285(1)	Cl1–Pd1–N1	90.26(5)
Pd1–Cl2	2.297(1)	N1–Pd1–N2	86.29(7)
Pd1–N1	2.023(2)	N2–Pd1–Cl2	92.57(5)
Pd1–N2	2.035(1)	Cl2–Pd1–Cl1	90.76(2)

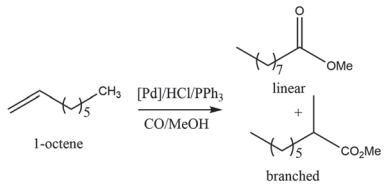

SCHEME 2 Methoycarbonylation of 1-octene catalyzed by palladium complexes 1–4.

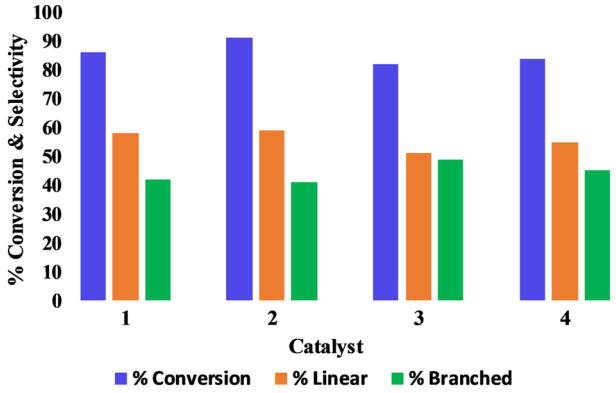

FIGURE 2 Methoxycarbonylation of 1-octene using complexes 1–4, time, 24 hr; temp, 90 °C; pressure, 60 bar; solvent, 50 ml toluene and 50 ml methanol; $Pd/PPh_3/HCl/1\text{-octene} = 1/2/10/200$

complexes **1** and **3** bearing smaller methyl substituents.[26] To the contrary, complex **3** gave slightly higher (49%) composition of branched esters compared to the 45% obtained for complex **4**, containing the bulkier phenyl group. A closer examination of the structures of complexes **1**–**4** may explain this lack of clear dependence of regioselectivity on the pyrazolyl substituents. From the solid state structures of complexes **1**, **2** and **4**, both the methyl and phenyl groups are facing away from the palladium atom, thus exerting little steric influence around the palladium center. In an effort to relate the degree of steric crowding by the ligands around the metal ion with the catalytic activity of the metal chelates, the steric shielding parameter, G_M^T (complex) was calculated using the program Solid G (Figure 3).[27] The data in Figure 3 shows that the more sterically bulky ligand (**L2**), bearing phenyl substituents on the pyrazol ring does not significantly increase the steric shielding of the metal center. For instance, using the analogous complexes **1** and **3**, ligands **L1** (Me) and **L2** (Ph) shields 70.64% and 73.87% of the Pd metal respectively. This relatively minor difference could thus explain the similar regioselectivities of the all the complexes.

2.4 | Influence of acid promoter and phosphine additive

Due to the superior catalytic activity of complex **2** in comparison to the other complexes, it was used for further investigations. First to be studied was the effect of acid promoters using inorganic, organic and Lewis acids (Table 3, entries 1–6). The role of the acid promoter in the methoxycarbonylaion reaction is believed to be the generation of the Pd-hydride, considered as the active species.[28,29] The most reactive acid was HCl (91%), while the organic acids, methyl sulfonic (MSA) and para-tolylsulfonic (*p*-TsOH) were inactive. This trend is similar to those found in literature and relates to the strength and coordinating abilities of the acids.[10,30] With respect to H_2SO_4, rapid decomposition of the active species due to its poor stabilizing ability, may account for its relative lower activity compared to HCl.[31]

Surprisingly, an opposite trend was reported using the Lewis acids $EtAlCl_2$ and $AlMe_3$, where the less Lewis acidic $AlMe_3$ (80%) was found to be more active compared to the more acidic $EtAlCl_2$ (72%). The reason for this observation is unclear to us at this time, though the ability to stabilize the active palladium species by the more basic acid promoter (better electron-donor) may be hypothesised. The identity of the acid promoter also influenced product composition. Most intriguing was the complete switch of regioselectivity towards the branched esters for $EtAlCl_2$ (81%) compared to the other acids (Table 3, entries 1–6). This points to the formation of a different active species for $EtAlCl_2$, which appears to promote a 2,1 insertion of the 1-octene substrate. No

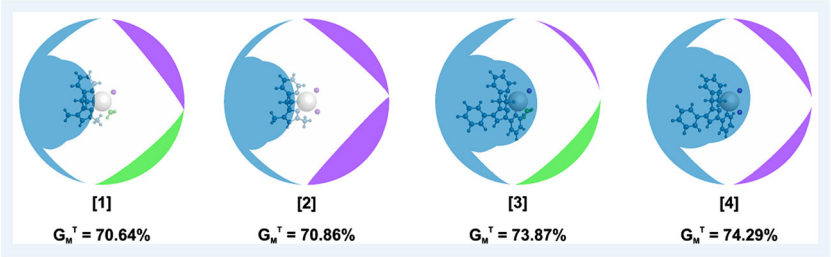

FIGURE 3 Illustration of the degree of steric shielding (%) of the metal ion surface, GMT (complex), for the palladium complexes 1–4. The blue shadow represents screening by the chelating pyrazol-pyridyl ligand; the green represents the methyl ligand and the purple the chloride ligands

TABLE 3 The effect of acid promoter and phosphine additive in the methoxycarbonylation of 1-octene[a]

Entry	Acid promoter	Phosphine additive	Conv. (%)[b]	l/b (%)[b]
1	HCl	PPh_3	91	59/41
2	H_2SO_4	PPh_3	70	51/49
3	$EtAlCl_2$	PPh_3	72	19/81
4	$AlMe_3$	PPh_3	80	56/44
5	HCl	[d]dPPe	16	33/67
6	HCl	[e]P $(Cy)_3$	37	36/64
7	HCl	P $(OMe)_3$	56	18/82
8	*p*-TsOH	PPh_3	trace	-
9	[c]MSA	PPh_3	trace	-

[a]Temp, 90 °C; solvent system, 50 ml toluene and 50 ml methanol; [Pd]/[PR_3]/[Acid]/1-octene]; 1/2/10/200; $P_{(CO)}$, 60 bar; time, 24 hr;

[b]Conversion of olefin to esters and ratio between linear and branched esters determined by GC.

[c]Methanesulfonic acid (MSA),

[d]1,2-bis (diphenylphosphino)ethane,

[e]tricyclohexylphosphine.

such report is can be found in literature, and further studies would be necessary to understand this phenomenon.

It has been widely reported that the use of different phosphine derivatives to stabilize the active palladium species significantly affect the catalytic performance of palladium complexes in methoxycarbonylation reactions.[32,33] Complex **2**, was thus used to probe this feature using both chelating and monodentate phosphine groups, offering various electronic and steric properties (Table 3, entries 1, 7–9). From the results, it was evident that monodentate phosphines gave higher conversions compared to the chelating phosphines. For example, conversions of 91% and 16% were observed for PPh_3 and dppe, respectively (Table 3, entries 1 *vs* 7). This may be associated with competition between the chelated phosphine ligand and the olefin substrate for the vacant active site.[32] With respect to steric bulk, the relatively sterically demanding PCy_3 afforded lower conversions of 37%, compared to the less bulkier PPh_3, which gave conversions of 91%. This trend may be assigned to a hindered substrate coordination to the palladium metal when the bulky PCy_3 phosphine is used.[33] In addition, we noted that the more electron rich P $(OMe)_3$ group resulted in lower percentage conversion (56%) compared to PPh_3 (91%). The lower reactivity reported for P $(OMe)_3$ can be understood to originate from reduced electrophilicity of the metal center, thus limiting substrate coordination.[23] The nature of the phosphine additive was also observed to confer some influence on the regioselectivity of the resultant catalysts. Consistent with previous findings,[34] changing from PPh_3 to P $(OMe)_3$ was followed by a drastic shift in the composition of the branched esters from 41% to 82% (Table 3, entries 1 and 9). This trend has been associated with minimal steric hindrance to give the bulkier branched esters.[35]

2.5 | Role of solvent in methoxycarbonlylation of 1-octene

The role played by the solvent system in regulating the catalytic behavior of the complexes in methoxycarbonylation of 1-octene was probed using different solvent systems and complex **2** (Figure 4). The best solvent system was the toluene/methanol mixture, which recorded 91%, while cyclohexane/methanol (19%) solvent combination gave the lowest conversion of 19%. The reduced conversion in cyclohexane/methanol could be apportioned to the low solubility of complex **2** in cyclohexane. This was supported by comparative activities witnessed in chlorobenzene and toluene solvents. On the other hand, the negative effect of DMSO solvent, which is more polar and expected to display better solubility, may be assigned to its enhanced coordination ability to the metal center. This has the potential to block olefin coordination, consistent with the observed diminished catalytic activities.[36–38] On the contrary, a change in the solvent system did not significantly influence the regioselectivity of the catalyst, affording between 54%–60% of the linear esters across the board. This is reasonable as there is no known role of the solvent in controlling the steric parameters of the active catalyst.

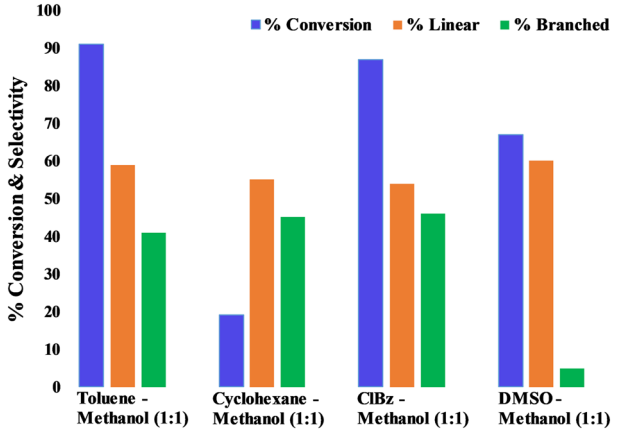

FIGURE 4 The effect of solvent system on percentage conversion and regioselectivity on methoxycarbonylation of 1-octene using complex 2; 2/PPh_3/HCl/1-octene; 1/2/10/200, temp, 90 °C; P (CO), 60 bar, time, 24 hr

2.6 | Effect of reaction conditions and olefin chain length

The next series of studies were carried out to investigate how changes in the reaction temperature, pressure, reaction time, catalyst loading and olefin chain length would affect the catalytic ability of complex **2** (Table 4). First, we lowered the reaction temperature from 90 °C to 60 °C and observed comparable conversions of 91% and 89% respectively (Table 4, entries 1 and 2). This depicts thermal stability of complex **2** at higher temperatures, and more importantly, good catalytic activities at lower temperatures. Reduction of the CO pressure from 40 bar, 50 bar to 60 bar led to a gradual decline in percentage conversion of complex **2** from 91%, 77% to 48% respectively (Table 4, entries 2, 4–5). This trend is not unusual and can be attributed to the diminished insertion of CO at lower pressures. However, there was no appreciable change in regioselectivity of complex **2** with change in both reaction temperature and pressure.

In order to establish the optimum catalyst concentration of complex **2**, the 1-octene/**2** ratio was varied from 100 to 400 corresponding to 1 mol% to 0.25 mol% respectively (Table 4, entries 1, 5–6). Decreasing the 1-octene/**2** ratio from 400 to 100 (increasing the catalyst concentration) appeared to increase the percentage conversions from 55% to 93%, respectively. However, this interpretation is deceptive upon critical analyses of the TOF values obtained. For instance, TOFs of 9.1 hr^{-1} and 3.9 hr^{-1} were observed at [1-octene/[**2**] ratios of 400 (0.25 mol%) and 100 (1 mol%), respectively (Table 4, entries 5 and 6). These results thus indicate that the increase in percentage conversions was not in the same order of magnitude with the increase in catalyst loadings. It is therefore conceivable, that using lower catalyst loadings of 0.25 mol% gives the best results qualitatively, in good agreement with reports of Zolezzi *et al.*[39] In terms of regioselectivity, we observed the formation of more branched esters (40%) at higher catalyst loadings of 1 mol% compared to 18% of the branched esters reported at 0.25 mol% (Table 4, entries 5 and 6). This could be attributed to enhanced isomerization reactions at higher catalyst loadings.[35,38]

Lastly, we studied the stability of complex **2** in the methoxycarbonylation of 1-octene by varying the reaction times from 12 hr to 36 hr using [1-octene]/[**2**] molar ratio of 200 (Table 4, entries 1, 7–9). Maximum TOF was obtained at shorter reaction times of 12 hr (7.7 hr^{-1}) and 24 hr (7.6 h^{-1}), while a significant decline at longer reaction time of 36 hr (5.3 hr^{-1}) was reported. The comparable TOF values at 12 hr and 24 hr indicate appreciable catalyst stability within this period, while a drop in TOF within 36 hr is evident of catalyst deactivation. Significantly, we noted a concomitant increase in the composition of the branched esters from 16% to 49% with increase in reaction time from 12 hr to 36 hr (Table 4, entries 7 and 9). This occurrence is not common in methoxycarbonylation reactions, though isomerization *via* 2,1 insertions may be implicated.[26]

Further investigations to establish the influence of olefin chain length on the catalytic performance of complex **2** were carried out using styrene, 1-octene, 1-nonene, and 1-decene (Figure 5). From Figure 5, the catalytic

TABLE 4 Effect of pressure, temperature, reaction time and catalyst loading on the methoxycarbonylation of 1-octene using complex **2**[a]

Entry	P_{CO}/ bar	T/ °C	Time/ hr	[2]/ [octene]	%Conv[b]	l/b[b]	TOF/ h^{-1}
1	60	90	24	1/200	91	58/42	7.6
2	60	60	24	1/200	89	59/41	7.4
3	40	90	24	1/200	48	55/45	4.1
4	50	90	24	1/200	77	57/43	6.4
5	60	90	24	1/100	93	60/40	3.9
6	60	90	24	1/400	55	82/18	9.1
7	60	90	12	1/200	46	74/16	7.7
8	60	90	32	1/200	94	55/45	5.9
9	60	90	36	1/200	99	51/49	5.5

[a]Temp, 90 °C; solvent system, 50 ml toluene and 50 ml methanol; [1-octene]/[HCl]/[PPh_3]/[Pd], 200/10/2/1; $P_{(CO)}$, 60 bar; time, 24 hr;

[b]Determined by GC.

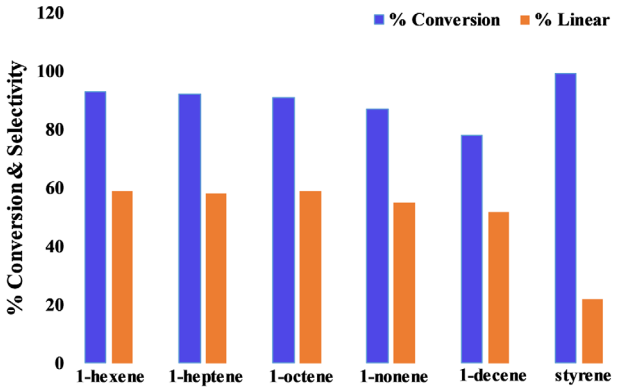

FIGURE 5 The effect of olefin substrate on percentage conversion and regio-selectivity towards linear esters using catalyst 2. Reaction conditions: temperature, 90 °C; 2/PPh_3/HCl/olefin, 1/2/10/200; Pressure (CO), 60 bar; time, 24 hr

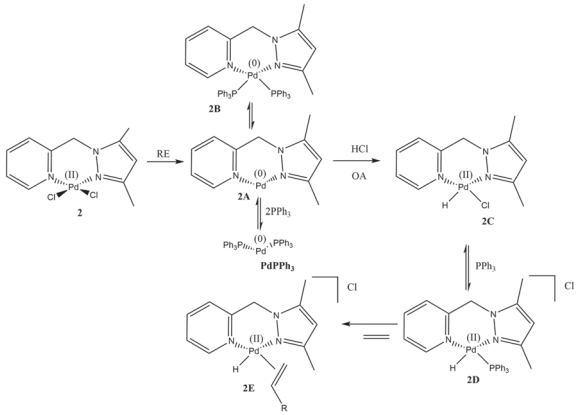

SCHEME 3 Proposed activation and stabilization pathways of complex 2 in the presence of HCl and triphenylphosphine, PPh_3.

activity of **2** was marginally influenced by the nature of the substrate. As an illustration, on changing from 1-hexene to 1-decene, a slight drop in percentage conversion from 93% to 78% was observed. This, somehow, contradicts our previous reports, where a significant decline in catalytic activity from 90% to 20% was observed for 1-hexene and 1-decene, respectively[15,34,40] and underscores the superiority of the current systems. The higher reactivity of styrene substrate is normal and can be linked to the generally more reactive benzylic palladium (II) intermediate in comparison to the alkyl palladium (II) species.[41] The identity of the substrate was found to marginally influence the regioselectivity of the ester products. For example, 41% and 48% of the branched esters were obtained for 1-hexene and 1-decene, respectively, consistent with increase in internal isomers with olefin chain length.[26] More intriguing was the drastic shift to 78% of the branched esters for styrene substrate, indicating that a 2,1 insertion mode was the preferred mode of styrene coordination to the metal atom.

2.7 | Determination of the role of PPh_3 by DFT studies

In order to establish the role played by the PPh_3 additive in the generation and stabilization of the active species in these methoxycarbonylation reactions, we simulated pre-catalyst **2**, and its various adducts [$Pd^{(0)}$(**L1**)] (**2A**), [$Pd^{(0)}$(**L1**)(PPh_3)$_2$] (**2B**), [$Pd^{(II)}$(**L1**)HCl] (**2C**) and [$Pd^{(0)}$(**L1**)(PPh_3)H] (2D). In addition, complex [$Pd^{(0)}$(PPh_3)$_2$] was computed to determine the possible displacement of ligand **L2** from the metal coordination sphere upon addition of excess PPh_3 ligand (Scheme 3). The simulations were performed with Gaussian 09 W using the CAM-B3LYP hybrid exchange-correlation functional using the Coulomb-attenuating method. The relative energies of the complex [Pd(**L2**)Cl_2] (**2**) and the intermediates were calculated as shown in Figure 6. The intermediate zerovalent complexes are significantly different in structure as the Pd(0) atom has a d^{10} electron configuration and therefore a strong preference for the formation of linear palladium complexes. This is in contrast to the square planar coordination geometry of the d^8 Pd (II) ion. This difference in electron configuration provides a likely explanation for why the [Pd (PPh_3)$_2$] complex is the lowest energy zerovalent complex. The soft metal ion will favor coordination to the soft *P*-donor ligands as opposed to the harder *N*-donor ligand. The bidentate nature of the *N*-donor ligand will also inhibit the formation of a linear complex and is hence higher in energy, in contrast to the monodentate P-donor ligands.

Compound **2b** proposes the coordination of two PPh_3 ligands and the bidentate N-donor ligand to the Pd(0) metal center to form a four-coordinate complex. Numerous attempts were made to simulate a plausible structure for a compound of this structure. These were all found to be unstable and reverted to the stable [Pd (PPh_3)$_2$] species and free ligand. This result is in agreement with literature, which shows that this is an unstable coordination geometry for Pd(0). A search of the Cambridge Structural Database (CSD) shows no reported structures of a Pd(0) complex with two triphenylphosphine ligands in a *cis* configuration and a bidentate *N*-donor ligand.[42] This alludes to the instability of complexes of this nature. There is a single example of a related complex with *cis*-PPh_3 ligands and *cis*-monodentate N-donor ligands,[43] where the monodentate nature of the coordinated ligands in this case makes this scenario possible.

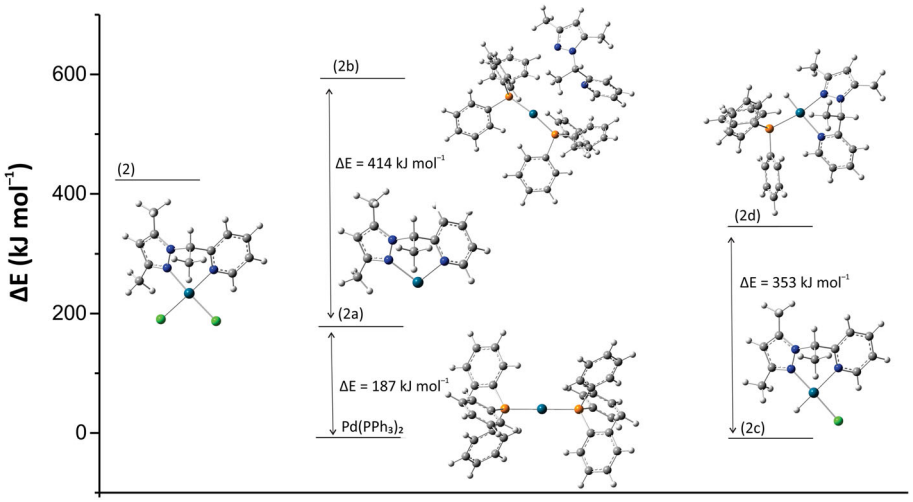

FIGURE 6 DFT simulation of the energies of the proposed intermediates for the activation and stabilization of the palladium complex (2) in the presence of PPh_3 and HCl

Thus, from the DFT calculated energies (Figure 6), it is clear that complex $[Pd^{(0)}(\mathbf{L1})(PPh_3)_2]$ (**2B**) is energetically unfavorable, hence unlikely to be the active species. While the $[Pd^{(0)}(PPh_3)_2]$, is very stable, this is unlikely to be the active species due to the strong Pd-N bonds, thus the (pyrazolylmethyl)pyridine ligand may be not easily displaced by the PPh_3 ligand. Additionally, the observation of the dependence of catalytic performance on complex structures/ligand motif, suggests that the active species contains the ligands, consistent with our recent NMR studies.[34] Thus from the DFT calculations, the mono-ligated PPh_3 compound $[Pd^{(0)}(\mathbf{L1})(PPh_3)Cl]$ (**2D**), may explain the role of the PPh_3 in stabilizing the active Pd hydride species. Even though the hydride compound $[Pd^{(0)}(\mathbf{L1})HCl]$ (**2C**), appears more stable, the addition of excess PPh_3 is likely to displace the Cl ligand to form **2D**. Indeed, the dependence of catalytic activities on the nature of the phosphine groups further supports the presence of **2D** as the active intermediate, consistent with the DFT results.

3 | CONCLUSIONS

In summary, four palladium (II) complexes supported by (pyrazolyethyl)pyridine ligands have been synthesized and structurally characterized. The complexes are monometallic in which the coordination sphere consists one bidentate pyrazolyl ligand and two auxiliary chloride/methyl ligands to give distorted square planar geometry. The complexes form active catalysts in the methoxycarbonylation of higher olefins to afford mainly linear esters. Solid angle modelling established similar steric environment around the metal atom in the complexes, consistent with the comparable regioselectivity towards linear esters. The nature of the acid promoter, phosphine additive and reaction conditions controlled the catalytic performance of the complexes. While increase in olefin chain length did not significantly alter the catalytic activity, it did influence product distribution. DFT studies show the possible formation of monophosphine stabilized palladium hydride species as the active intermediate.

4 | EXPERIMENTAL SECTION

4.1 | General materials and instrumentation

All manipulations were carried out under a nitrogen atmosphere using standard Schlenk techniques. The solvents used; absolute ethanol (≥96%), diethylether (≥99%) and toluene (≥99.8%) were of analytical grade and were dried over sodium and distilled prior to use. While dichloromethane (≥99.8%) was dried and distilled over P_2O_5 respectively. Reagents, 3,5-dimethylpyrazole (99% purity), 1,5-cyclooctadiene (≥99%), 1,3-diphenyl-1,3-propanedione (98%), tetrabutylammonium bromide (≥99%), sodium hydroxide (≥98%), sodium borohydride (≥99%), 2-acetylpyridine (≥99%), palladium (II) chloride (≥99%) and thionyl chloride (≥99%) were obtained from Sigma Aldrich and used as received. Ligands 2-[1-(3,5-dimethylpyrazol-1-yl)ethyl]pyridine (**L1**) and 2-[1-(3,5-diphenylpyrazol-1-yl)ethyl]pyridine (**L2**) were prepared following our recently published procedures.[16] NMR spectra were recorded on a Bruker Ultrashield 400

instrument (^{1}H NMR 400 and 500 MHz, ^{13}C NMR 100 MHz) in DMSO-d_6 and $CDCl_3$ solutions at room temperature. Chemical shifts are reported in δ (ppm) and referenced to the residual $CHCl_3$ in $CDCl_3$. Coupling constants are measured in Hertz (Hz). Elemental analyses were performed using CHNS-O Flash 2000 Thermoscientific analyser. Mass spectra were recorded on an LC Premier micro-mass spectrometer while infrared spectra were obtained using Spectrum 100 FT-IR spectrometer.

4.2 | Syntheses of pyrazolyl palladium (I) complexes 1–4

4.2.1 | [{2-(3,5-dimethylpyrazol-1-yl) ethylpyridine}PdClMe] (1)

To a solution of Pd (COD)MeCl (0.10 g, 4.96 mmol) in diethylether (15 ml) was added a solution of 2-[1-(3,5 ;dimethylpyrazol-1-yl)ethyl]pyridine, **L1**, (0.13 g, 4.96 mmol) in diethyl ether (10 ml) to form a light yellow precipitate. The resultant mixture was stirred for 24 hr and filtered to give a light yellow solid. Recrystallization of the crude product from a mixture of CH_2Cl_2: hexane (2:1) gave single crystals suitable for X-ray analysis. Yield: 0.65 g (58%).^{1}HNMR ($CDC1_3$, δ, ppm): 0.95 (s, 3H, Pd-CH_3), 2.34 (s, 3H, pz-CH_3); 2.68 (s, 3H, pz-CH_3); 1.94 (d, 3H, $^3J_{HH}$ = 8.9, -CH-CH_3); 5.67 (q, 1H, $^3J_{HH}$ = 6.7, CH_3-C-*H*); 6.92 (s, 1H, pz-*H*); 7.29 (d, 1H, $^3J_{HH}$ = 7.8, 3-py-*H*); 7.32 (dd, 1H, $^3J_{HH}$ = 7.8, 5-py-*H*); 7.79 (td, 1H, $^3J_{HH}$ = 7.9, 4-py-*H*); 8.52 (d, 1H, $^3J_{HH}$ = 8.0, 6-py-*H*). ^{13}C-NMR ($CDC1_3$, δ, ppm): δ 11.9 (pz-CH_3), 15.1 (pz-CH_3), 23.0 (Pd-CH_3), 25.2 (CH-CH_3), 58.7 (CH_3-CH), 107.40 (4-pz-*C*), 122.82 (5-py-*C*), 124.7 (3-py-*C*), 138.4 (4-py-*C*), 140.2 (2-pz-*C*), 151.2 (6-py-*C*), 152.2 (5-pz-*C*), 155.5 (2-py-*C*). MS (ESI): *m/z* (%) = 308.05 [M + Na]$^+$, 100%). FT-IR: $\nu_{C=N(pz)}$ = 2162 cm^{-1}, $\nu_{C=N(py)}$ = 1980 cm^{-1}. Anal. Calcd for $C_{13}H_{18}ClN_3Pd$: C, 43.59; H, 5.07; N, 11.73. Found: C, 43.76; H, 5.28; N, 11.44.

4.2.2 | [{2-(3,5-dimethylpyrazol-1-yl) ethylpyridine}$PdCl_2$] (2)

To a solution of [Pd (COD)Cl_2] (0.10 g, 4.96 mmol) in dichloromethane (10 ml) was added a solution of **L1** (0.13 g, 4.96 mmol) in dichloromethane (10 ml) and the resultant orange solution was stirred for 24 hr. After the reaction period, the solution was concentrated to about 5 ml and layered with hexane (5 ml). The mixture was then kept at 4 °C to afford yellow single crystals suitable for X-ray analysis. Yield: 0.55 g (48%). ^{1}H NMR (DMSO, δ, ppm): 2.45 (3H, s, pz-CH_3); 2.44 (3H, s, pz-CH_3); 2.94 (d, 3H, $^3J_{HH}$ = 8.75, -CH-CH_3); 5.51 (s, H, pz-CH_3); 6.17 (q, 1H, $^3J_{HH}$ = 7.90, CH_3-C-*H*); 7.61 (dd, 1H, $^3J_{HH}$ = 7.4, 5-py-*H*); 8.12 (td, 1H, $^3J_{HH}$ = 7.74, 4-py-*H*); 7.92 (d, 1H, $^3J_{HH}$ = 7.48, 3-py-*H*); 8.88 (d, 1H, $^3J_{HH}$ = 7.94, 6-py-*H*). ^{13}C NMR (DMSO, δ, ppm): 11.7 (pz-CH_3), 15.24 (pz-CH_3), 23.2 (CH-CH_3), 58.2 (CH_3-CH), 108.2 (3-pz-*C*), 125.8 (5-py-*C*), 126.1 (3-py-*C*), 141.6 (4-py-*C*), 143.3 (2-pz-*C*), 152.1 (6-py-*C*), 154.16 (4-pz-*C*), 156.1 (2-py-*C*). MS (ESI): *m/z* (%) = 401.98 ([M + Na]$^+$, 100%). FT-IR: $\nu_{C=N(pz)}$ = 2164 cm^{-1}, $\nu_{C=N(py)}$ = 2112 cm^{-1}. Anal. Calcd for $C_{12}H_{15}Cl_2N_3Pd$: C, 38.07; H, 3.99; N, 11.10. Found: C, 38.15; H, 3.97; N, 10.87.

4.2.3 | [{2-(3,5-diphenylpyrazol-1-yl) ethylpyridine}PdClMe] (3)

Complex **3** was prepared following the procedure described for **1** using [Pd (COD)MeCl] (0.10 g, 4.96 mmol) and **L2** (0.14 g, 4.96 mmol). Recrystallization of the crude product by slow diffusion of hexane into a CH_2Cl_2 solution gave **3** as an analytically pure compound. Yield: 0.18 g (53%).^{1}H-NMR ($CDC1_3$,δ, ppm): 2.20 (s, 3H, Pd-CH_3); 2.99 (d, 3H, $^3J_{HH}$ = 8.8, CH-CH_3); 5.77 (q, 1H, $^3J_{HH}$ = 6.6, CH_3-C*H*); 6.54 (s, 1H, pz-C*H*); 7.46 (dd, 1H, $^3J_{HH}$ = 7.8, 5-py-C*H*), 7.13 (d, 1H, $^3J_{HH}$ = 7.7, 3-py-C*H*); 7.46 (m, 2H, Ph); 7.77 (m, 4H, Ph), 7.79 (td, 1H, $^3J_{HH}$ = 7.7, 4-py-C*H*); 8.27 (m, 4H, Ph); 9.25 (d, 1H, $^3J_{HH}$ = 7.6, 6-py-C*H*), ^{13}C NMR ($CDC1_3$, δ, ppm): 13.7 (Pd-CH_3), 23.2 (CH-CH_3), 59.7 (CH_3-C*H*), 107.5 (3-pz-*C*H), 122.9 (5-py-*C*H), 124.9 (3-py-*C*H), 128.2 (2-Ph-C*H*), 128.42 (2-Ph-C), 128.73 (6-ph-C), 128.86 (6-Ph-*C*H), 129.07 (3-Ph-*C*H), 129.12 (3-Ph-*C*H), 129.30 (5-Ph-*C*H), 129.38 (5-Ph-*C*H), 129.64 (4-Ph-*C*H), 130.1 (4-ph-C), 134.1 (1-Ph-*C*), 135.1 (4-py-*C*H), 146.2 (6-py-*C*-N), 155.2 (4-pz-C), 156.3 (6-py-*C*=N). MS (ESI): *m/z* (%) =483 (M^+, 100%). FT-IR: $\nu_{C=N(pz)}$ = 2162 cm^{-1}, $\nu_{C=N(py)}$ = 1606 cm^{-1}. Anal. Calcd for $C_{23}H_{22}ClN_3Pd$: C, 57.28; H, 4.60; N, 8.71. Found: C, 57.55; H, 4.43; N, 8.80.

4.2.4 | [{2-(3,5-Diphenylpyrazol-1-yl) ethylpyridine}$PdCl_2$] (4)

Complex **4** was prepared following the procedure described for **2** using [Pd (COD)Cl_2] (0.10 g, 4.96 mmol) and **L2** (0.14 g, 4.96 mmol). Recrystallization from hexane/CH_2Cl_2 solvent system at 4 °C produced orange single crystals suitable for X-ray analysis. Yield: 0.15 g (44%).^{1}H NMR (DMSO, δ, ppm): 3.29 (d, 3H, $^3J_{HH}$ =8.6, CH-CH_3); 5.73 (q, 1H, $^3J_{HH}$ = 6.4, CH_3-C*H*); 6.56

(s, H, pz-C*H*); 7.27 (d, 1H, $^3J_{HH}$ = 7.6, 3-py-C*H*); 7.43 (dd, 1H, $^3J_{HH}$ = 7.8, 5-py-C*H*); 7.48 (m, 2H, Ph), 7.64 (td, 1H, $^3J_{HH}$ = 7.7, 4-py-C*H*), 7.62 (m, 4H, PH), 8.27 (m, 4H, Ph); 9.35 (d, H, $^3J_{HH}$ = 7.6, 6-py-C*H*). ^{13}C NMR (DMSO, δ, ppm): 20.2 (CH-*C*H$_3$), 52.2 (CH$_3$-*C*H), 108.1 (3-pz-*C*H), 124.1 (5-py-C*H*), 125.7 (3-py-*C*H), 127.6 (2-Ph-*C*H), 128.3 (2-Ph-*C*H), 128.4 (Ph-*C*H), 130.61 (Ph-*C*H), 130.9 (Ph-*C*H), 134.0 (4-py-*C*H), 144.9 (2-pz-*C*-CH$_3$), 146.9 (6-py-*C*H), 154.79 (4-pz-*C*H), 155.3 (2-py-*C*N). MS (ESI): *m/z* (%) =503 (M^+, 10%). FT-IR: $\nu_{C=N(pz)}$ = 2164 cm^{-1}, $\nu_{C=N(py)}$ = 1605 cm^{-1}. Anal. Calcd for $C_{22}H_{19}Cl_2N_3Pd$: C, 52.56; H, 3.81; N, 8.36. Found: C, 52.38; H, 3.99; N, 8.19.

4.3 | X-ray crystallography

The Pd (II) complexes were all isolated as yellow needle-like crystals. X-ray data were recorded on a Bruker Apex Duo equipped with an Oxford Instruments Cryojet operating at 100(2) K and an Incoatec microsource operating at 30 W power. Crystal and structure refinement data are given in Table 1. The data were collected with Mo Kα (λ = 0.71073 Å) radiation at a crystal-to-detector distance of 50 mm. Data were collected using omega and phi scans with exposures taken at 30 W X-ray power and 0.50° frame widths using APEX2.[44] The data were reduced with the program SAINT[44] using outlier rejection, scan speed scaling, as well as standard Lorentz and polarization correction factors. A SADABS semi-empirical multi-scan absorption correction[44] was applied to the data. Direct methods, SHELX-2016[45] and WinGX,[46] were used to solve the data. All non-hydrogen atoms were located in the difference density map and refined anisotropically with SHELX-2016.[45] All hydrogen atoms were included as idealized contributors in the least squares process, with C-H$_{aromatic}$ distances of 0.93 Å and U_{iso} = 1.2 Ueq, C-H$_{methine}$ distances of 1.00 Å and U_{iso} = 1.2 Ueq and C–H$_{methyl}$ distances of 0.98 Å and U_{iso} = 1.5 Ueq. Platon SQUEEZE[47] was used to remove disordered solvent from the lattice of complex **4**. This process left solvent accessible voids of 205.57 Å^3; 16.7% of the unit cell volume.

4.4 | Density functional theory calculations

Density functional theory (DFT) simulations were performed using Gaussian 09W[48] using the PBE hybrid functional.[49,50] A split basis set was applied in the simulations, this split basis set specified the 6-311G level of theory[51,52] for the C, H, Cl and N atoms and the LanL2DZ (which makes use of effective core potentials) basis set for the palladium (II) ion.[53–55] The X-ray coordinates of the metal chelates **1**, **2** and **4** were used for input structures. Normal geometry convergence criteria were applied and no symmetry constraints imposed. The input files were prepared using GaussView 5.0; the same program was used to analyze the output files. Structural overlays were performed using Mercury 3.10.[42]

4.5 | Methoxycarbonylation catalysis procedure

The methoxycarbonylation experiments using complexes **1**–**4** as catalysts were performed in a high pressure Parr reactor equipped with a temperature control unit, cooling system, internal stirrer and a sampling valve. In a typical experiment, complex **2** (0.012 g, 0.06 mmol), PPh_3 (0.03 g, 0.12 mmol), HCl (0.02 mL, 0.60 mmol) and 1-octene (2.00 mL, 12.00 mmol) corresponding to [Pd]/[PPh_3]/[HCl]/[1-octene] ratio of 1:2:10:200 were dissolved in a mixture of methanol (50 ml) and toluene (50 ml). The reactor was then evacuated and the catalytic solution was introduced to the reactor *via* a cannula. The reactor was purged three times with CO, then heated at the required temperature. The desired pressure was then set and the reaction stirred at 500 rpm for the entire duration of the experiment. At the end of the reaction time, the reaction was cooled, excess CO vented off and the samples drawn for GC analysis to determine the percentage conversion of the alkene substrate to esters. A typical sample for GC analyses was prepared by passing it through a microfilter into a GC vial. GC–MS analyses were run under the following standard chromatography conditions: −25 m CPSil 19 capillary column, 1.2 mm film thickness, Helium carrier column gas 5 psi, injector temperature 250 °C, oven program 50 °C for 4 mins rising to 200 °C at 20 °C/min and holding at 200 °C. The percentage conversions were determined by comparing the peak areas of the reactants and total products, assuming 100% mass balance. The identities of the ester products were assigned using standard authentic samples and mass spectral data.

SUPPLEMENTARY INFORMATION

Supplementary materials contain additional NMR and IR spectroscopic spectral data, mass spectra of the palladium complexes and X-ray crystallography files. The CCDC data entries for the structures are CCDC: 1884240,

1884241, 1884242 and 1884243 for compounds **L2**, **1**, **2** and **4**, respectively.

ACKNOWLEDGMENTS

The authors are grateful to the NRF-DST (South Africa) Centre of Excellence in Catalysis (c*change, OLE-10.3-UKZN,) National Research Foundation - South Africa (CPRR-98938) and the University of KwaZulu-Natal for financial support.

ORCID

Stephen O. Ojwach https://orcid.org/0000-0001-5309-4926

REFERENCES

[1] C. F. J. Barnard, *Organometallics* **2008**, *27*, 5402.

[2] C. Bianchini, G. Giambastiani, I. G. Rios, G. Mantovani, A. Meli, A. M. Segarra, *Coord. Chem. Rev.* **2006**, *250*, 1391.

[3] S. D. Ittel, L. K. Johnson, M. Brookhart, *Chem. Rev.* **2000**, *100*, 1169.

[4] D. Wang, D. Astruc, *Chem. Rev.* **2015**, *115*, 6621.

[5] H. H. Voge, C. R. Adams, in *Advances in Catalysis*, (Eds: D. D. Eley, H. Pines, P. B. Weisz) Vol. 17, Academic Press, Cambridge, United Kingdom, **1967**, 151.

[6] R. F. Heck, J. P. Nolley, *J. Org. Chem.* **1972**, *37*, 2320.

[7] N. Miyaura, A. Suzuki, *Chem. Rev.* **1995**, *95*, 2457.

[8] G. Kiss, *Chem. Rev.* **2001**, *101*, 3435.

[9] G. J. Harkness, M. L. Clarke, *Eur. J. Org. Chem.* **2017**, *2017*, 4859.

[10] V. de la Fuente, M. Waugh, G. R. Eastham, J. A. Iggo, S. Castillón, C. Claver, *Chem. – A. Eur. J.* **2010**, *16*, 6919.

[11] C. Bianchini, A. Meli, W. Oberhauser, M. A. Zuideveld, Z. Freixa, P. C. J. Kamer, A. L. Spek, O. V. Gusev, A. M. Kal'sin, *Organometallics* **2003**, *22*, 2409.

[12] P. A. Aguirre, C. A. Lagos, S. A. Moya, C. Zuniga, C. Vera-Oyarce, E. Sola, G. Peris, J. C. Bayon, *Dalton Trans.* **2007**, 5419.

[13] A. Seayad, S. Jayasree, K. Damodaran, L. Toniolo, R. V. Chaudhari, *J. Organomet. Chem.* **2000**, *601*, 100.

[14] S. O. Ojwach, J. Darkwa, *Inorgan. Theor. Chim. Acta* **2010**, *363*, 1947.

[15] M. G. Alam, T. A. Tshabalala, S. O. Ojwach, *J. Surfactant Deterg.* **2017**, *20*, 75.

[16] M. N. Magubane, M. G. Alam, S. O. Ojwach, O. Q. Munro, *J. Mol. Struct.* **2017**, *1135*, 197.

[17] W. M. Motswainyana, S. O. Ojwach, M. O. Onani, E. I. Iwuoha, J. Darkwa, *Polyhedron* **2011**, *30*, 2574.

[18] W. M. Motswainyana, M. O. Onani, S. O. Ojwach, B. Omondi, *Inorg. Chim. Acta* **2012**, *391*, 93.

[19] G. S. Nyamato, S. O. Ojwach, M. P. Akerman, *Organometallics* **2015**, *34*, 5647.

[20] K. J. Akerman, C. Venter, L. A. Hunter, M. P. Akerman, *J. Mol. Struct.* **2015**, *1091*, 74.

[21] L. C. Spencer, I. A. Guzei, T. V. Segapelo, J. Darkwa, *Act. Cryst. Sec. E.* **2012**, *68*, m317.

[22] K. J. Kilpin, J. D. Crowley, *Polyhedron* **2010**, *29*, 3111.

[23] L. K. Johnson, C. M. Killian, M. Brookhart, *J. Am. Chem. Soc.* **1995**, *117*, 6414.

[24] K. Kumar, J. Darkwa, *Dalton Trans.* **2015**, *44*, 20714.

[25] V. Goudy, A. Jaoul, M. Cordier, C. Clavaguéra, G. Nocton, *J. Am. Chem. Soc.* **2017**, *139*, 10633.

[26] A. V. Smarun, W. Shahreel, S. Pramono, S. Y. Koo, L. Y. Tan, R. Ganguly, D. Vidović, *J. Organomet. Chem.* **2017**, *834*, 1.

[27] I. A. Guzei, M. Wendt, *Dalton Trans.* **2006**, 3991.

[28] C. Zúñiga, S. A. Moya, P. J. C. L. Aguirre, *Catal. Lett.* **2009**, *130*, 373.

[29] L. Crawford, D. J. Cole-Hamilton, M. Bühl, *Organometallics* **2015**, *34*, 438.

[30] D. B. Williams, M. L. Shaw, M. J. Green, C. W. Holzapfel, *Angew. Chem. Int. Ed.* **2008**, *47*, 560.

[31] C.-M. Tang, X.-L. Li, G.-Y. Wang, *Korean J. Chem. Eng.* **2012**, *29*, 1700.

[32] X.-F. Wu, H. Neumann, M. Beller, *Chem. Rev.* **2013**, *113*, 1.

[33] C. Arderne, L. A. Guzei, C. W. Holzapfel, T. Bredenkamp, *ChemCatChem* **2016**, *8*, 1084.

[34] T. A. Tshabalala, S. O. Ojwach, *Trans. Met. Chem.* **2018**, *43*, 339.

[35] J. A. Fuentes, J. T. Durrani, S. M. Leckie, L. Crawford, M. Bühl, M. L. Clarke, *Cat. Sci. Technol.* **2016**, *6*, 7477.

[36] H. Ünver, F. Yılmaz, *Catalysts* **2016**, *6*, 147.

[37] P. J. Dyson, P. G. Jessop, *Cat. Sci. Technol.* **2016**, *6*, 3302.

[38] F. Yılmaz, A. Mutlu, H. Ünver, M. Kurtça, İ. Kani, J. Supercrit, *Fluids* **2010**, *54*, 202.

[39] S. Zolezzi, S. A. Moya, G. Valdebenito, G. Abarca, J. Parada, P. Aguirre, *Appl. Organomet. Chem.* **2014**, *28*, 364.

[40] T. A. Tshabalala, S. O. Ojwach, M. A. Akerman, *J. Mol. Catal. A: Chem.* **2015**, *406*, 178.

[41] P. K. Santra, P. Sagar, *J. Mol. Catal. A: Chem.* **2003**, *197*, 37.

[42] C. F. Macrae, I. J. Bruno, J. A. Chisholm, P. R. Edgington, P. McCabe, E. Pidcock, L. Rodriguez-Monge, R. Taylor, J. van de Streek, P. A. Wood, *J. Appl. Cryst.* **2008**, *41*, 466.

[43] A. Romerosa, C. López-Magaña, M. Saoud, S. Mañas, E. Colacio, J. Suárez-Varela, *Inorg. Chim. Acta* **2000**, *307*, 125.

[44] A. Bruker, *SAINT and SADABS*, Bruker AXS Inc., Madison, WI, USA **2012**.

[45] G. Sheldrick, *Acta Cryst. Sec. C* **2015**, *71*, 3.

[46] L. Farrugia, *J. Appl. Cryst.* **2012**, *45*, 849.

[47] A. Spek, *Act. Cryst. Sec. D* **2009**, *65*, 148.

[48] G. W. Trucks, M. J. Frisch, H. B. Schlegel, G. E. Scuseria, M. A. Robb, J. R. Cheeseman, G. Scalmani, V. Barone, B. Mennucci, G. A. Petersson, H. Nakatsuji, M. Caricato, X. Li, H. P. Hratchian, A. F. Izmaylov, J. Bloino, G. Zheng, J. L. Sonnenberg, M. Hada, M. Ehara, K. Toyota, R. Fukuda, J. Hasegawa, M. Ishida, T. Nakajima, Y. Honda, O. Kitao, H. Nakai, T. Vreven, J. A. Montgomery, Jr., J. E. Peralta, F. Ogliaro, M. Bearpark, J. J. Heyd, E. Brothers, K. N. Kudin, V. N. Staroverov, R. Kobayashi, J. Normand, K. Raghavachari, A. Rendell, J. C. Burant, S. S. Iyengar, J. Tomasi, M. Cossi, N.

Rega, J. M. Millam, M. Klene, J. E. Knox, J. B. Cross, V. Bakken, C. Adamo, J. Jaramillo, R. Gomperts, R. E. Stratmann, O. Yazyev, A. J. Austin, R. Cammi, C. Pomelli, J. W. Ochterski, R. L. Martin, K. Morokuma, V. G. Zakrzewski, G. A. Voth, P. Salvador, J. J. Dannenberg, S. Dapprich, A. D. Daniels, Ö. Farkas, J. B. Foresman, J. V. Ortiz, J. Cioslowski, D. J. Fox, Gaussian, Inc., Wallingford CT, **2009**.

[49] J. P. Perdew, K. Burke, M. Ernzerhof, *Phys. Rev. Lett.* **1996**, *77*, 3865.

[50] J. P. Perdew, K. Burke, M. Ernzerhof, *Phys. Rev. Lett.* **1997**, *78*, 1396.

[51] A. D. McLean, G. S. Chandler, *J. Chem. Phys.* **1980**, *72*, 5639.

[52] R. Krishnan, J. S. Binkley, R. Seeger, J. A. Pople, *J. Chem. Phys.* **1980**, *72*, 650.

[53] P. J. Hay, W. R. Wadt, *J. Chem. Phys.* **1985**, *82*, 270.

[54] P. J. Hay, W. R. Wadt, *J. Chem. Phys.* **1985**, *82*, 299.

[55] W. R. Wadt, P. J. Hay, *J. Chem. Phys.* **1985**, *82*, 284.

SUPPORTING INFORMATION

Additional supporting information may be found online in the Supporting Information section at the end of the article.

How to cite this article: Zulu S, Alam MG, Ojwach SO, Akerman MP. Structural and theoretical studies of the methoxycarbonylation of higher olefins catalysed by (Pyrazolyl-ethyl) pyridine palladium (II) complexes. *Appl Organometal Chem*. 2019;e5175. https://doi.org/10.1002/aoc.5175